

## Crystallographic, hyperfine and magnetic characterization of a maraging-400 alloy

T. J. B. Alves<sup>1</sup> · G. C. S. Nunes<sup>1</sup> · P. W. C. Sarvezuk<sup>2</sup> ·  
F. F. Ivashita<sup>1</sup> · A. M. H. de Andrade<sup>3</sup> · A. Viegas<sup>4</sup> ·  
A. Paesano Jr.<sup>1</sup>

© Springer International Publishing Switzerland 2017

**Abstract** Maraging400-like alloys were made by arc-melting iron with the alloy elements (i.e., Ni, Co, Ti and Mo), followed by a high temperature heat-treatment for solubilization. The solubilized alloys were further heat-treated (480 °C and 580 °C, by 3 h), for aging. The samples were finely characterized by X-ray diffraction (Rietveld refinement), Mössbauer spectroscopy and magnetization techniques. The results revealed that the as-solubilized sample is martensitic and ferromagnetic. Its residual induction and coercive field increase monotonically with the maximum applied field of a magnetization minor loop and both curves presented very similar shapes. The area of the minor loops varies parabolically with this maximum applied field. The aging induced an atomic rearrangement in the martensite phase, involving change in the composition and lattice parameters, reversion of austenite and the formation of the Fe<sub>3</sub> Mo<sub>2</sub> intermetallic compound. Comparisons are presented between the results obtained by us for these alloys and those obtained for Maraging-350 steel samples.

---

**Electronic supplementary material** The online version of this article (doi:10.1007/s10751-017-1418-6) contains supplementary material, which is available to authorized users.

---

This article is part of the Topical Collection on *Proceedings of the 15th Latin American Conference on the Applications of the Mössbauer Effect (LACAME 2016), 13–18 November 2016, Panama City, Panama* Edited by Juan A. Jaén

---

✉ A. Paesano Jr.  
andrea.paesano@pq.cnpq.br

<sup>1</sup> Universidade Estadual de Maringá, Maringá, Brazil

<sup>2</sup> Universidade Tecnológica Federal do Paraná, Campo Mourão, Brazil

<sup>3</sup> Universidade Federal do Rio Grande do Sul, Porto Alegre, Brazil

<sup>4</sup> Universidade Federal de Santa Catarina, Florianópolis, Brazil

**Keywords** Maraging-400 · Martensite · Austenite · Rietveld method · Mössbauer spectroscopy · Magnetic properties

## 1 Introduction

Maraging steels constitute a family of low-carbon high alloy steels, having as main alloying elements Ni (18wt%), Co, Ti and Mo and, sometimes, Al or Cr [1, 2]. They are magnetic steels and present ultra-high strength and are divided into sub-classes – 200, 250, 300, 350 and 400, according to their yield strength (in ksi) [3]. These materials have several applications such as in sporting equipment, aeronautic components and hysteresis motors [1, 2].

The metallurgical routine of its fabrication involves, after the proper fusion alloying, a solubilization step – usually performed in the 82 °C – 1050 °C range - to dissolve the alloy elements in the iron austenite matrix [2–4]. The steel is then cooled to room temperature (RT), in time varying from minutes to a few hours. This temperature path leads to a martensitic transformation of which the final product is a metastable structure, with the alloy elements forming an extended solid solution in iron. Formerly, these steels were supposed to crystallize in the *bcc* structure, but recent studies showed that the true structure is tetragonal [5].

Heat treatments in the 480 °C – 580 °C temperature range – a process of so-called *aging* - induce changes in the local chemical composition and may even favor the precipitation of intermetallic compounds. The tribological, mechanical or magnetic properties may be thus modified, according to several studies [4, 6, 7]. The magnetic hardening of these steels is one of the most striking effects of the aging [8].

A number of results, regarding the structural and magnetic changes that occur because of an aging treatment, have been reported previously for some of these steels [9–11]. However to the best of our knowledge, the Maraging-400 steel has not been crystallographically (i.e., by Rietveld refinement) and magnetically characterized before. Only studies on mechanical properties appear reported in literature [12].

In addition to presenting the largest yield strength among the Maraging steels, Maraging-400 also has the highest cobalt content [13]. These features make it very stimulating to describe the physical properties of the material and compare them with those of the rest of the Maraging family.

In this sense, we are currently conducting an investigation aiming to characterize the crystalline structure and magnetic properties of a Maraging400-like alloy, solubilized and heat-treated. This work has been done by X-ray diffraction, Mössbauer spectroscopy and magnetometry techniques applied on specimens carefully prepared for characterization, in order to avoid (or minimize) mechanical effects that may induce phase transformations.

In this paper, we present the first results obtained on solubilized and heat-treated alloys of the Maraging-400 type, prepared with high purity metals. Comparisons are presented between the results obtained for these alloys and those obtained for Maraging-350 steel samples.

## 2 Experimental

The Maraging400-like alloy was made by arc-melting iron with the alloy elements (i.e., Ni, Co, Ti and Mo), and the concentrations are shown in Table 1. The resultant button (~ 1 g) was re-melted at least three times, aiming to maximize the sample homogeneity.

**Table 1** Chemical composition of the Maraging400-like alloy [13]

ALLOY ELEMENTS	WT%
Nickel	13.0
Cobalt	15.0
Molybdenum	10.0
Titanium	0.2

Then, slices ( $\phi \lesssim 1$  mm) were taken from the re-melted button, in a precise metallographic cutter with a diamond saw. These plates with rounded contours, were heat treated under argon atmosphere at 1050 °C for 1 h, for solubilization. Further, they were manually sanded on both sides, with 100, 600 and 1200 sandpaper. Part of these samples was heat treated at 480 °C and 580 °C, for periods of 3 h and, then, finely polished again on one of the sides.

Immediately after sanding or polishing, solubilized and heat treated samples were characterized by X-ray diffraction at room temperature, using Co  $K \alpha$  radiation ( $\lambda = 1.788970$  Å), in a conventional diffractometer, in  $\theta$ - $2\theta$  Bragg-Brentano geometry. The  $2\theta$  range was from 40° to 130°, with 0.02° increments and a counting time of 8 seconds per step. The FULLPROF program [14] was applied to refine the crystalline structure by the Rietveld method, considering the  $Fm-3m$  space group for the austenitic phase and  $I4$  for martensitic phase, as conducted for Maraging-350 samples [15]. A pseudo-Voigt shape function was used to fit the experimental data. The refined data were the lattice parameter, the peak shape and isotropic thermal parameters.

After taking the diffraction measurements, the plates were further sanded until they reached  $\sim 60$   $\mu\text{m}$  thickness and used for Mössbauer spectroscopy. After that, a small disk  $\sim 3$  mm in diameter was cut from each of the thinnest plates and used to take magnetization measurements.

Transmission Mössbauer spectra were taken at RT, with a  $^{57}\text{Co}(\text{Rh})$  source of 50 mCi activity, moved with constant acceleration, using as absorbers the foils described above. The spectrometer was calibrated with metallic iron ( $\alpha$ -Fe foil) at RT. The numerical fits were made considering a Lorentzian line shape and applying the criterion of the minimum chi-square. The isomer shift, quadrupole splitting, hyperfine magnetic field, individual linewidths and  $A_2/A_3$  area ratio were free to vary. The  $A_2/A_3$  ratios of the magnetic discrete components were constrained to be the same, whereas the  $A_1/A_3$  ratios were always kept fixed (i.e. = 3).

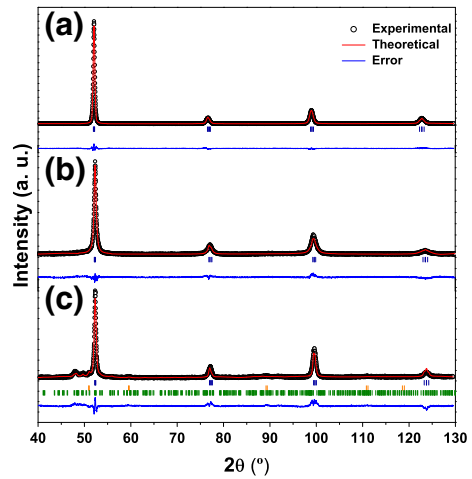
The magnetization -  $M(\text{emu}/\text{cm}^3)$  - vs. applied magnetic field -  $H_{\text{ap}}(\text{Oe})$  - curves were taken at RT, in a vibrating sample magnetometer (VSM) with  $10^{-5}$  emu sensitivity. Starting with the sample at zero magnetization, minor loops were extracted until the magnetic saturation of the sample was reached. Magnetic induction -  $B(\text{T})$  - as a function of the true magnetic field (i.e.,  $H = H_{\text{ap}} - N_{\text{d}} \cdot M$ ) was calculated considering the demagnetizing factor ( $N_{\text{d}} = 0.33$ ) of the specimen used in the magnetic measurement.

### 3 Results and discussions

#### 3.1 X-ray diffractometry

Figure 1 shows the refined diffractograms of the solubilized 480 °C / 3 h and 580 °C / 3 h heat treated samples. The diffractometric profile of the solubilized sample (Fig. 1a) is

**Fig. 1** Refined diffractograms for the as-solubilized (a), 480 °C / 3 h (b) and 580 °C / 3 h (c) heat-treated Maraging-400 alloys; | Martensite; | Austenite; | Fe<sub>3</sub>Mo<sub>2</sub>



characteristic of a monophasic alloy and corresponds to the martensite phase, similar to those found for other solubilized maraging steels [5, 10]. Performing a close inspection, no extra peaks could be identified, which means that no secondary phase is present in a significant amount (i.e., in the resolution limits of the X-ray diffraction technique).

The diffractogram of the 480 °C / 3 h aged sample (Fig. 1b) does not reveal any significant qualitative modification compared to that of Fig. 1a, exception regarding the original position and some enlargement of the peaks. In contrast, the diffractogram of the 580 °C / 3 h aged sample (Fig. 1c) shows peaks of secondary phases. Some of them may be attributed to the (reverted) austenite, whereas others belong to a Fe<sub>3</sub>Mo<sub>2</sub>-like intermetallic compound or  $\mu$  phase (sg. *R-3h*) [16, 17].

It is worth noting that the occurrence of the Fe<sub>2</sub>Mo Laves phase (sg. *P63/mmc*) precipitates in heat-treated Maraging steels is frequently reported in literature, usually detected by TEM experiments (EDS and electron diffraction) [18]. Nonetheless, their presence has never been identified by X-ray diffraction, possibly due to its quite small volume fraction. Trials to refine the diffractogram of Fig. 1c, considering the structure of a Laves phase and, also, the sg. *R-3mh* (which is sometimes attributed to the Fe<sub>7</sub>Mo<sub>6</sub> compound [16]) did not work at all. Diffractograms of samples prepared recently, under harder aging conditions, confirm the crystallization of the sg. *R-3h* structure. These diffractometric profiles are currently being analyzed and will be published elsewhere.

The refined lattice parameters obtained from the diffractograms of Fig. 1 are shown in Table 2.

In comparison with those determined for commercial Maraging-350 samples [15], the lattice parameters of the martensite phase obtained here are a little bit longer, possibly consequence of the higher concentration of larger atoms in the Maraging400 alloy (i.e., Mo). However,  $a$  and  $c$  decrease for the heat-treated samples because of the depletion of the molybdenum content in martensite, as a direct consequence of the Fe<sub>3</sub>Mo<sub>2</sub> precipitation. Possibly, other Mo-containing compounds may have precipitated (e.g., Ni<sub>3</sub>(Mo, Ti)), although in minor amounts, as earlier observed, even in aged Maraging-350 steels [19]. The presence of Mo-rich precipitates is one of the reasons pointed out for the extraordinary hardness of the Maraging-400 steel. Actually, the high molybdenum content of this steel seems to change all the dynamics of phase transformation and precipitation during aging [12] and great differences in their magnetic properties are expected, in comparison to those of the Maraging-350 steel.

**Table 2** Lattice parameters of the phases identified in the as-solubilized and heat treated samples

Sample	Phase	Structure	Lattice Parameters (Å)
as-solubilized	Martensite	Tetragonal ( s.g. $I4$ )	$a = b = 2.8889$ (2) $c = 2.8745$ (3)
480 °C / 3 h	Martensite		$a = b = 2.8782$ (3) $c = 2.8637$ (5)
580 °C / 3 h	Martensite		$a = b = 2.8751$ (2) $c = 2.8616$ (3)
	Austenite	Cubic ( s.g. $Fm-3m$ )	$a = 3.6043$ (2)
	Fe <sub>3</sub> Mo <sub>2</sub>	Rhombohedral( s.g. $R-3h$ )	$a = b = 10.989$ (3) $c = 19.607$ (2)

The lattice parameters obtained for austenite are, in general, consistent with previously reported data [19].

### 3.2 Mössbauer spectroscopy

The Mössbauer spectra of the solubilized and aged samples are shown in Fig. 2. The spectrum of the as-solubilized sample (Fig. 2a) clearly reveals an entirely magnetic material similar to other non-aged Maraging steels [5, 20, 21]. This pattern is assigned to martensite phase based on the X-ray diffractogram and our earlier work on the solution annealed Maraging-350 steel [5].

The spectrum reveals the presence of different magnetic components, which means that iron has different atomic neighborhoods in martensite, in spite of the alloy phase homogeneity. For the purpose of numerical analysis, these components could be separated into three groups, according to the hyperfine magnetic field values. Therefore, the fit was performed considering three discrete sextets, likewise conducted for a commercial Maraging-350 sample [5]. As reported earlier, on the solid solutions of iron with other metals [22], cobalt and nickel contribute to increase the hyperfine magnetic field, relative to the value of an iron matrix (i.e., 330 kOe). Thus, Sextet 1 could be attributed to the Co-Ni richest region, whereas Sextet 3 would come from the Co-Ni poorest region, if any. Obviously, Sextet 2 would be respective to a region of intermediary Co-Ni concentrations.

The 480 °C / 3 h and 580 °C / 3 h spectra (Fig. 2b and c) present a magnetic fraction plus a central unsplit contribution, similarly to other aged Maraging steels [15, 21, 23]. They were fitted considering three discrete sextets and a singlet. The paramagnetic (PM) contribution (i.e., the singlet), which was not observed for the as-solubilized sample, may be attributed mainly to (reversed) austenite – its single line pattern is very well established [15] – and, according to the X-ray diffraction, to the Fe<sub>3</sub>Mo<sub>2</sub> compound. The PM character of the Fe<sub>3</sub>Mo<sub>2</sub> phase may be presumed from earlier reports [24, 25]. Whereas the former phase was identified also in aged Maraging-350 samples, the latter was not [15].

Besides the Fe<sub>3</sub>Mo<sub>2</sub> intermetallic compound pointed out above, the Ni<sub>3</sub> (Ti, Mo) phase has also been identified in aged samples [19] and this phase could, plausibly, be present here (with iron dissolved in the A<sub>3</sub> B matrix) though in a small amount. The large singlet linewidth is evidence for multiple sites but it is not possible to separate the PM components.

It is worth noting that the X-ray diffractogram of the 480 °C / 3 h sample does not reveal any phase other than martensite, whereas the corresponding Mössbauer spectrum shows another unequivocal spectral contribution. This may be explained by recalling that the Mössbauer is a “microscopic” technique. Besides being selective for iron, it is able to identify and quantify phases from small crystallites (eventually, nanostructured) while X-ray diffraction only sees “larger” crystallites. This is exactly the great achievement of the

**Fig. 2** Mössbauer spectra for the as-solubilized (a), 480 °C / 3 h (b) and 580 °C / 3 h (c) heat-treated Maraging-400 alloys; — Sextet 1; — Sextet 2; — Sextet 3

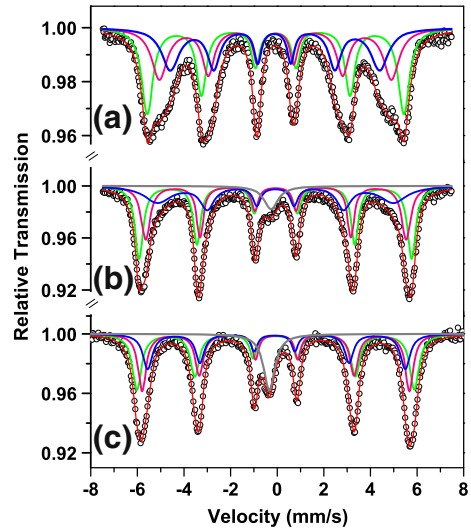


**Table 3** Hyperfine parameters and subspectral areas, for the solubilized and aged samples

Sample	Site	$\delta$ (mm/s) ( $\pm 0.01$ )	$2\varepsilon$ (mm/s) ( $\pm 0.01$ )	$B_{\text{hf}}$ (T) ( $\pm 0.2$ )	$\Gamma$ (mm/s) ( $\pm 0.02$ )	Area (%) ( $\pm 0.5$ )
<i>As-solubilized</i>	Sextet 1	0.04	0.00	34.1	0.43	38.7
	Sextet 2	0.03	0.00	30.9	0.40	32.2
	Sextet 3	0.00	0.03	27.9	0.37	29.1
	Singlet	—	—	—	—	—
480 °C / 3 h	Sextet 1	0.04	-0.02	36.3	0.39	37.6
	Sextet 2	0.05	0.02	34.7	0.35	30.5
	Sextet 3	0.04	0.00	31.4	0.40	26.9
	Singlet	-0.15	—	—	0.73	5.0
580 °C / 3 h	Sextet 1	0.03	0.02	36.9	0.37	35.0
	Sextet 2	0.07	-0.04	35.6	0.32	31.5
	Sextet 3	0.04	0.08	34.3	0.34	22.9
	Singlet	-0.23	—	—	0.64	10.6

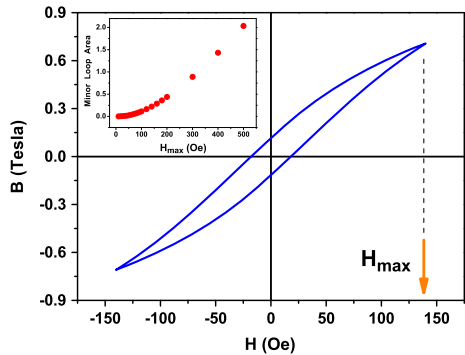
$\delta$  = isomer shift;  $2\varepsilon$  = quadrupole splitting;  $B_{\text{hf}}$  = hyperfine magnetic field;  $\Gamma$  = linewidth of the line 3(4);

$^{57}\text{Fe}$  Mössbauer spectroscopy technique, which affords a fine characterization where iron alloys and compounds are present.

The fitted hyperfine parameters and subspectral areas for the samples characterized in this investigation are shown in Table 3.

Analyzing the hyperfine parameters, we can see that the isomer shifts ( $\delta$ 's) of the martensite phase are close to zero, as usual for this phase. The quadrupole splitting is nearly zero for all sites, for all samples, reflecting the symmetry of the iron sites, which is very close to the cubic, in either the martensite or the austenite phases. This is somewhat intriguing, especially for martensite which shows a tetragonal distortion and where, as well as for austenite, the iron sites present different configurations of nearest neighbors.

**Fig. 3** Magnetic induction *vs.* applied magnetic field curve of a minor loop, for the as-solubilized Maraging-400 alloy; in this case,  $H_{max} = 140$  Oe. Insert: area of a minor loop (in  $10^7 \cdot \text{Gauss} \cdot \text{Oe}$ ) *vs.*  $H_{max}$



It can also be seen that the  $B_{hf}$  values of the heat-treated samples increase considerably relative to that of the  $B_{hf}$  of the as-solubilized sample.

This growth in  $B_{hf}$  provides evidence that an alteration takes place around the iron atoms because of the heat treatment, without changing the crystallographic structure of the martensite. The alteration may be described as a progressive enrichment of nickel and/or cobalt atoms around the iron, which must contribute positively to the  $B_{hf}$  [22].

However, according to the metastable phase diagram proposed by Schmidt et al. for the Fe-Ni system [3], reversed austenite has a higher nickel concentration than martensite in aged samples, although this superiority diminishes increasing the temperature of the aging process (see Fig. 2a of ref. 3). Thus, it can be inferred that cobalt is the element most grouped around iron atoms during the aging process and is the main agent responsible for increasing  $B_{hf}$ . Cobalt atoms in the iron neighborhood even compensate for some reduction in the nickel concentration in martensite, thus justifying why  $B_{hf}$  increases with aging.

The linewidths ( $\Gamma$ 's) also change with the aging, decreasing significantly. This means that the heat treatment reduces the number of configurations around the iron atoms, while the nearest neighborhood becomes richer in cobalt atoms.

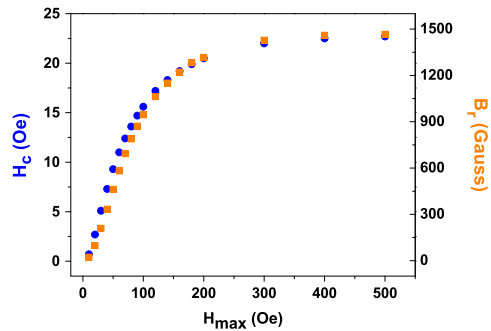
### 3.3 Magnetic characterization of the as-solubilized sample

Figure 3 shows one of the minor loops – i.e., curves of the magnetic induction ( $B$ ) as a function of the applied magnetic field ( $H$ ), before reaching saturation, for the solubilized sample.

The curve reveals a hysteresis, typical of a ferromagnetic material, with a far larger area than that obtained for a solubilized Maraging-350 steel, at the same maximum field [5]. The insert shows the variation with  $H_{max}$  of the minor loop area. The parabolic shape of this curve is recurrently found for as-solubilized and aged Maraging steels. Its  $a$ ,  $b$  and  $c$  parameters seem to be linked to the specific aging conditions applied for a sample, according to preliminary analyzes on similar curves of aged samples (results not shown).

Figure 4 shows the coercive field ( $H_c$  / left ordinate) and the residual induction ( $B_r$  / right ordinate), as functions of  $H_{max}$ , obtained from the minor loops measured until  $H_{max} = 500$  Oe. The curves are very similar in shape: at the beginning, there is a linear variation, with  $H_c$  ( $B_r$ ) increasing at the rate  $\sim 12\%$  ( $\sim 1125\%$ ). Beyond  $H_{max} = 100$  Oe,  $H_c$  ( $B_r$ ) bends and tends asymptotically to 23 Oe (1460 Gauss), at reaching the saturation induction. The values found for  $H_c$  ( $B_r$ ) are larger ( $\sim 7x / \sim 25x$ ) than those found earlier for a solubilized Maraging-350 sample [5].

**Fig. 4** Coercive field (blue balls) and residual induction (orange squares) vs.  $H_{\max}$ , for the as-solubilized Maraging-400 alloy



## 4 Conclusions

- The as-solubilized Maraging400-like alloy is martensitic, with tetragonal crystalline structure, and ferromagnetic, similar to the Maraging-350 steel;
- Its residual induction and coercive field increase monotonically with the maximum applied field of a magnetization minor loop and both curves present very similar shapes;
- The area of the minor loops varies parabolically with  $H_{\max}$ ;
- The magnetic properties -  $H_C$ ,  $B_r$  and Minor loop area, as a function of  $H_{\max}$  - of the as-solubilized Maraging400-like alloy behave similarly to those of the as-solubilized Maraging-350 steel, although reaching higher values (particularly, for  $B_r$ ) in the whole 0 - 500 Oe range of  $H_{\max}$ ;
- Heat-treating the alloy for 3 h in the range 480 °C – 580 °C produces an atomic rearrangement in the martensite phase, involving change in the composition and lattice parameters;
- Aging also induces the austenite reversion and precipitation of the  $Fe_3Mo_2$  intermetallic compound; whereas the reversion is common, the compound precipitation is not usually detected in aged Maraging-350 steel samples.

**Acknowledgments** The authors want to thank the Brazilian foundation CAPES (Edital Pró-Estratégia 50/2011 – Projeto 3) for supporting this research.

## References

1. Decker, R.F.: Notes on the Development of Maraging Steels. In: Source Book on Maraging Steels XI-XV (1979)
2. Magnée, A., Drapier, J.M., Dumont, J., Coutsouradis, D., Habraken, L.: Cobalt-Containing High-Strength Steels, Bruxelles: Centre D'information du Cobalt (1974)
3. Schmidt, M., Rohrbach, K.: Heat Treating of Maraging Steels. In: ASM Handbook: Heat Treating 528-548 (1991)
4. Floreen, S., Speich, G.R.: Some Observations Strength and Toughness of Maraging Steels. In: Source Book on Maraging Steels 327-336 (1979)
5. Nunes, G.C., Sarvezuk, P.W., Biondo, V., Blanco, M., Nunes, M.V.S., Andrade, A.M.H., Paesano Jr., A.: Structural and magnetic characterization of martensitic Maraging-350 Steel. *J. Alloys Compd.* **646**, 321-325 (2015)
6. Mei, P.R., Costa e Silva, A.L.D.: Aços e ligas especiais (1988)
7. Guo, Z., Li, D., Sha, W.: Quantification of precipitate fraction in maraging steels by X-ray diffraction analysis. *J. Mater. Sci. Technol.* **20**, 126-130 (2004)



8. Tavares, S.S.M., da Silva, M.R., Neto, J.M., Pardal, J.M., Fonseca, M.P.C., Abreu, H.F.G.: Magnetic properties of a Ni–Co–Mo–Ti maraging 350 steel. *J. Alloys Compd.* **373**(1), 304–311 (2004)
9. Viswanathan, U.K., Dey, G.K., Asundi, M.K.: Precipitation hardening in 350 grade maraging steel. *Metall. Trans. A* **24**, 2429–2442 (1993)
10. Pardal, J.M.: Aço Maraging classe 300: Propriedades mecânicas e magnéticas em diversas condições de tratamento térmico São Paulo (2012)
11. Habiby, F., Siddiqui, T.N., Hussain, H., Ul Haq, A., Khan, A.Q.: Lattice changes in the martensitic phase due to ageing in 18 wt% nickel maraging steel grade 350. *J. Mater. Sci. Lett.* **31**, 305–309 (1996)
12. Padial, A.G.F.: Caracterização Microestrutural do aço Maraging de Grau 400 de resistência mecânica Ultraelevada Tese - Instituto de Pesquisas energéticas e Nucleares são Paulo SP (2002)
13. Mihalisin, J.R., Bieber, C.G.: Progress toward attaining theoretical strength with iron-nickel maraging steel. *J. Metals* **18**, 1033–1036 (1966)
14. Rodríguez-Carvajal, J.: FULLPROF: A Program For Rietveld Refinement and Pattern Matching Analysis at the Satellite Meeting on Powder Diffraction of the XV IUCr Congress 127 (1990)
15. Nunes, G.C.S., Sarvezuk, P.W.C., Alves, T.J.B., Biondo, V., Ivashita, F.F., Paesano Jr., A.: Maraging-350 steel: Following the aging through diffractometric, magnetic and hyperfine analysis. *J. Magn. Magn. Mate.* **421**, 457–461 (2017)
16. Sinha, A.K., Bruckley, R.A., Hume-Rothery, W.: Equilibrium diagram of the iron-molybdenum system. *J. Iron Steel Inst.* **205**, 191–195 (1967)
17. Van Der Kraan, A.M., Buschow, K.H.J.: The  $^{57}\text{Fe}$  Mössbauer isomer shift in intermetallic compounds of iron. *Phys. Rev. B* **138**, 55–62 (1986)
18. Zhu, F., Yin, Y.F., Faulkner, R.G.: Microstructural control of maraging steel c300. *J. Mater. Sci. Technol.* **27**(1), 395–405 (2011)
19. Tewari, T.R., Mazumder, S., Batra, I.S., Dey, G.K., Banerjee, S.: Precipitation in 18 wt% Ni maraging steel of grade 350. *Acta. Mater.* **48**, 1187–1200 (2000)
20. Li, X., Yin, Z., Li, H.: Mössbauer study of the 430 °C decomposition of 18Ni(350) maraging steel. *J. Mater. Sci. Lett.* **15**(4), 314–316 (1996)
21. Li, X., Yin, Z.: Mössbauer study of the aging behavior of 18Ni(350) maraging steel. *Mater. Lett.* **24**, 235–238 (1995)
22. Vincze, I., Campbell, I.A.: Mössbauer measurements in iron based alloys with transition metals. *J. Phys. F: Metal Phys.* **3**, 647–663 (1973)
23. Li, X.D., Yin, Z.D., Li, H.B., Lei, T.C., Liu, M.L., Liu, X.W., Jin, M.Z.: Mössbauer study of the early stages of aging in 18Ni(350) maraging steel. *Mater. Chem. Phys.* **33**(3–4), 277–280 (1993)
24. Marcus, H.L., Fine, M.E., Schwartz, L.H.: Mössbauer-effect Study of Solid-Solution and Precipitated F-Rich Fe-Mo Alloys. *J. Appl. Phys.* **38**, 4750–4758 (1967)
25. Pickardt, B.: Dissertation, inst. Phys. Chem. Hamburg (2003)